DOI: 10.19884/j.1672-5220.202406011

Dynamic Characteristic Analysis and Structural Optimization of Entire Double-Shaft-Driven Needle Punching Machine for C/C Crucible Preforms

SUN Zhihong[1*], DENG Qicai[1], QU Zhiyang[1], WANG Zhenxi[2], WANG Bing[2], ZHANG Xi[1], ZHANG Jingzhang[2]

1. College of Mechanical Engineering, Donghua University, Shanghai 201620, China
2. Hangchen Shijiazhuang New Materials Technology Co., Ltd., Shijiazhuang 051432, China

Abstract: Double-shaft-driven needle punching machine is a specialized equipment designed for processing C/C crucible preforms. Its main needle punching module is operated by two sets of reciprocating crank-slider mechanisms. The intense vibration during needle punching not only generates huge noise, but also substantially reduces the quality of the preform. It is imperative to perform a dynamic analysis and optimization of the entire needle punching machine. In this paper, the three-dimensional (3D) model of the entire double-shaft-driven needle punching machine for C/C crucible preforms is established. Based on the modal analysis theory, the modal characteristics of the needle punching machine under various operating conditions are analyzed and its natural frequencies and vibration modes are determined. The harmonic response analysis is then employed to obtain the amplitude of the needle plate at different frequencies, and the structural weak points of the needle punching machine are identified and improved. The feasibility of the optimized scheme is subsequently reevaluated and verified. The results indicate that the first six natural frequencies of the machine increase, and the maximum amplitude of the needle plate decreases by 70.3%. The enhanced dynamic characteristics of the machine significantly improve its performance, enabling more efficient needle punching of C/C crucible preforms.

Keywords: needle punching machine; dynamic characteristic; modal analysis; harmonic response analysis; structural optimization

CLC number: TH164 **Document code**: A

Article ID: 1672-5220(2025)04-0399-10

Open Science Identity (OSID)

0 Introduction

According to statistics, more than 95% of the basic materials used in the information technology industry are made of silicon crystalline materials[1]. At present, single-crystal silicon is mostly made by the direct drawing method[2] and the single-crystal furnace is used in the production process. C/C crucible has become one of the important parts of the single-crystal furnace owing to its good stability, high impact resistance and resistance to thermal shock[3]. The C/C crucible preform is mostly made by the method of needle punching. The movement mechanism of the needle punching machine mainly consists of a reciprocating crank-slider mechanism. During the production process, severe vibration is generated, which affects the quality of needle punching and produces huge noise.

To solve the balance problem of needle punching machines for producing non-woven fabrics, Tong[4] proposed a double-shaft-driven needle punching machine, theoretically capable of offsetting horizontal unbalanced force, thereby reducing machine vibration and simplifying processing and installation. Xu[5] pointed out that the vibration of the needle punching machine frame primarily arose from the inertial force generated by the reciprocating motion of the needle beam components, with the frame's amplitude correlating to the needle punching speed. As this speed increases, the frame's amplitude increases and then decreases beyond a certain threshold. The amplitude at the needle punching position has yet to be investigated. Zhong et al.[6] investigated the resonance problem generated by the needle punching process of the needle punching machine through on-site measurements and finite element simulation. They pointed out that the deformation of the needle beam was affected by the inertial force during the needle punching process, but only analyzed a single needle beam component. Yun[7] used the finite element simulation to investigate the modal characteristics of the engine bracket and proposed that the finite element prestressed modes had high computational accuracy, which could provide a basis for stiffness optimization. Zhang[8] analyzed the dynamic characteristics of the machine tool feed system and pointed out that mechanical structural parameters had a certain influence on the natural frequency of the system.

Received date: 2024-06-28

Foundation item: Open Project of Shanghai Key Laboratory of Lightweight Composite, China (No. 2232021A4-04)

* Correspondence should be addressed to SUN Zhihong, email: zhsun@dhu.edu.cn

Citation: SUN Z H, DENG Q C, QU Z Y, et al. Dynamic characteristic analysis and structural optimization of entire double-shaft-driven needle punching machine for C/C crucible preforms[J]. *Journal of Donghua University (English Edition)*, 2025, 42(4): 399-408.

As the position of the components changes, the natural frequency of the system changes significantly. Xie[9] conducted a modal analysis and harmonic response analysis on the connecting rod, crankshaft and needle beam in the crank-slider mechanism of the single-axis-driven needle punching machine. Moreover, the resonance parts were found, which provided a basis for the improvement of the vibration characteristics of the needle punching machine. However, only the dynamic characteristics of some components were analyzed, and the dynamic characteristics of the entire needle punching machine were not analyzed.

At present, most of the dynamic characteristics analysis and research on the needle punching machine for C/C crucible preforms are only focused on a single part or partial component. There is still relatively little research on the dynamic characteristics of the entire needle punching machine. The simplicity of the single part and partial component fails to capture the actual vibration within the entire system, especially the coupling effects between components. However, the modal analysis of the entire machine can more comprehensively consider a variety of factors under the actual working conditions, so as to more accurately assess the dynamic characteristics of the system. Therefore, the dynamic characteristics of the entire double-shaft-driven needle punching machine for C/C crucible preforms are studied. The research can provide an effective reference for the design of related needle punching machines and the study of dynamic characteristics.

1 Model Establishment of Entire Needle Punching Machine

1.1 Structure of entire needle punching machine

As shown in Fig. 1, the entire needle punching machine for C/C crucible preforms primarily comprises a frame, a main needle punching module, a core mold rotational support module, and an auxiliary needle punching module. The main needle punching module is driven by two sets of mechanisms that rotate synchronously in opposite directions, achieving the function of reciprocating movement of the needle punching components up and down. It requires two sets of crank-slider mechanisms to work together. The main needle punching module as a whole is height-adjusted by four lead screw modules suspended at the top of the frame to adapt to changes in the diameter of preforms. The core mold rotational support module is located below the main needle punching module. It is used to support and rotate the preform core mold and C/C crucible preform, as well as to realize station switching for easy loading and unloading of the core mold and other materials. The auxiliary needle punching module is located on the right side of the main needle punching module. Its needle punching part has three degrees of freedom for moving in the horizontal plane and rotating around the vertical axis. This ensures that the needles can consistently pierce vertically into the surface of the crucible, enabling the needle punching of the crucible bottom.

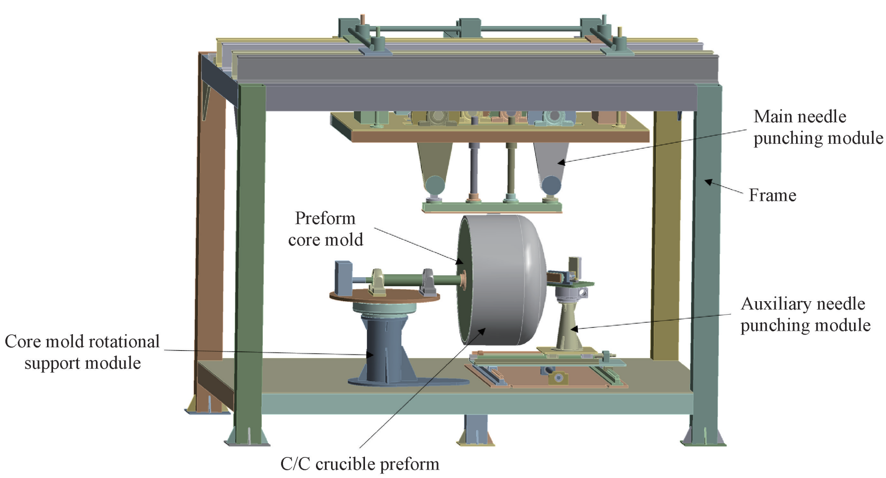

Fig. 1 Structure of entire needle punching machine for C/C crucible preforms

In the needle punching machine, the modular design is employed, and the needles remain perpendicular to the surface of the preform. This needle punching machine ensures the high molding quality of the preform and can simultaneously needle punch both the crucible body and the crucible bottom, thereby achieving a high production efficiency.

1.2 Establishment of finite element model of entire needle punching machine

SolidWorks 3D modeling software (Dassault Systèmes, USA) is utilized to create a three-dimensional (3D) virtual model of the needle punching machine for crucible preforms, which is subsequently imported into ANSYS Workbench (ANSYS, USA) to develop a finite element model. The overall model of the needle punching machine is very complex, including hundreds of parts, various chamfers, mounting holes and other features. Moreover, there are nonlinear connections such as slide rail drives, ball drives, belt drives and other nonlinear connections between the parts, which greatly increase the computational complexity of the modal analysis. The classical modal analysis theory is linear. Furthermore, there are numerous motors that present additional challenges in establishing an accurate finite element model. To enhance the accuracy and computational efficiency of the finite element model without altering the main structure, appropriate simplifications are made. Structural details with minimal impact on dynamic characteristics, such as threaded holes and rounded corners, are simplified. Ball drives and belt drives are omitted, and motors are replaced with mass blocks. ANSYS Workbench provides five contact types to realize the connection function, and each contact surface type is set as "bonded".

The establishment of the finite element model of the entire needle punching machine mainly includes the definition of material properties, meshing and boundary condition settings.

Firstly, it is necessary to define the material properties in the pre-processing stage, and the main material parameters of each part are shown in Table 1.

Secondly, the adaptive meshing technique is used. It optimizes the mesh type and size based on model characteristics, ensuring a high mesh quality with minimal computational demand. The maximum mesh cell size is set at 30 mm, considering the dimensions of various components. The local mesh is optimized. After meshing, the model comprises 1 375 714 nodes and 380 737 cells, reflecting an excellent overall mesh quality.

Finally, since the needle punching machine frame is fixed to the ground through the ground bolts in actual production, fixed constraints are imposed on the lower surface of the six frame bases. The simplified finite element model of the entire needle punching machine is shown in Fig. 2.

Table 1 Material properties for finite element model of entire needle punching machine for C/C crucible preforms

Material	Elastic modulus/Pa	Poisson's ratio	Density/ (kg/m^3)
Structural steel	2.00×10^{11}	0.300	7 850
HT200	1.48×10^{11}	0.310	7 200
QT400	1.61×10^{11}	0.274	7 010
Q235-A	2.12×10^{11}	0.288	7 860
45	2.09×10^{11}	0.269	7 890
Oak	2.23×10^{10}	0.374	936

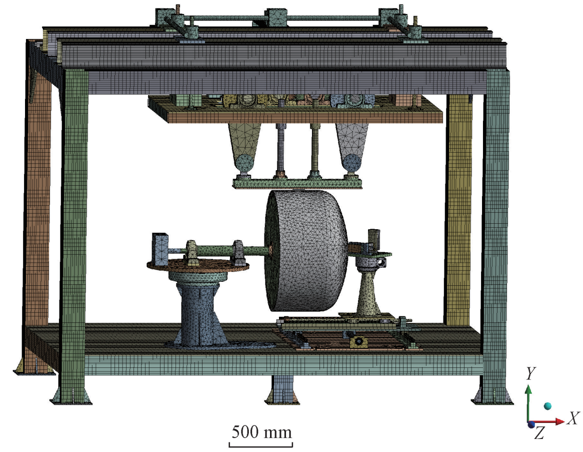

Fig. 2 Simplified finite element model of entire needle punching machine

2 Dynamic Characterization Analysis of Entire Needle Punching Machine

2.1 Modal analysis of entire needle punching machine

2.1.1 Principles of modal analysis

The modal analysis could examine the dynamic performance of a mechanical structure to determine the vibration characteristics of structural components, i. e., the natural frequency and vibration mode. For a defined structure, the corresponding generalized equation of motion for structural dynamics is[10-12]

$$\boldsymbol{M}\ddot{\boldsymbol{x}} + \boldsymbol{C}\dot{\boldsymbol{x}} + \boldsymbol{K}\boldsymbol{x} = \boldsymbol{F}(t), \quad (1)$$

where $\boldsymbol{M}$ represents the mass matrix of the system; $\boldsymbol{C}$ represents the damping matrix of the system; $\boldsymbol{K}$ represents the stiffness matrix of the system; $\ddot{\boldsymbol{x}}$ represents the acceleration vector; $\dot{\boldsymbol{x}}$ represents the velocity vector; $\boldsymbol{x}$ represents the displacement vector; $\boldsymbol{F}(t)$ represents the dynamic load applied to the system; t represents the time.

For free vibration and without damping,

$$\boldsymbol{M}\ddot{\boldsymbol{x}} + \boldsymbol{C}\dot{\boldsymbol{x}} = 0. \quad (2)$$

For a linear system, i. e., $\boldsymbol{M}$ and $\boldsymbol{K}$ are constants, free vibration as simple harmonic motion leads to

$$\boldsymbol{x} = \boldsymbol{\varphi}_i \cos(\omega_i t), \quad (3)$$

where $\boldsymbol{\varphi}_i$ represents an eigenvector; ω_i represents the natural frequency (eigenvalue) of the ith order mode.

The fundamental equation typically solved for the undamped modal analysis is the classical issue of eigenvalue:

$$\boldsymbol{K}\boldsymbol{\varphi}_i = \omega_i^2 \boldsymbol{M}\boldsymbol{\varphi}_i. \quad (4)$$

Solving Eq. (4) yields several solutions, i. e., the natural frequency of free vibration of the structure:

$$\omega_1 \leqslant \cdots \leqslant \omega_i = \sqrt{\frac{K_i}{M_i}} \leqslant \cdots \leqslant \omega_n, \quad (5)$$

where M_i represents the equivalent mass of the ith order mode; K_i represents the equivalent stiffness of the ith order mode.

2.1.2 Results of modal analysis for entire needle punching machine

The modal analysis can determine the natural frequency and vibration pattern of the entire needle punching machine for C/C crucible preforms without considering external conditions. Improvements based on this analysis can prevent the structure from resonating at specific frequencies and avert potential damage to the mechanism. Therefore, ensuring the stability of the needle punching machine through the modal analysis is crucial[13]. Modes have an infinite number of orders, but lower-order modes play a major role in the vibration of the mechanical structure, as the response induced by the higher-order modes decays rapidly[14]. Therefore, the first six orders of modes are the focus of research.

The shape, size, stiffness and loading mode of a structure in the modal analysis can all affect its natural frequencies and modes. During the entire processing cycle of the preform, the positions of each module in the needle punching machine vary, resulting in changes in the structural dimensions. The change in structural dimensions will directly affect the overall quality and stiffness distribution of the machine, thereby affecting the natural frequency. Throughout the entire processing cycle of the preform, the varying positions of each module in the needle punching machine impact the machine's overall modal state. The main needle punching module, which adjusts its height in response to changes in the preform's diameter, experiences significant positional shifts and is thus the primary focus of this study. The modal analysis of the entire needle punching machine is conducted with the main needle punching module positioned at both the lowest and highest workstations. Additionally, the modal analysis considers the position changes of the main needle beam, that is, the movement position changes of the crank-slider mechanism driven by the hyperbolic handle slider mechanism. The results of these analyses are shown in Table 2.

Table 2 The first six natural frequencies of entire needle punching machine at different positions of main needle punching module

Position		Natural frequency/Hz					
		1st order	2nd order	3rd order	4th order	5th order	6th order
The highest workstation	Needle beam at the highest position	7.86	8.05	18.15	18.60	19.37	19.54
	Needle beam at the lowest position	7.85	8.05	18.14	18.61	19.37	19.54
The lowest workstation	Needle beam at the highest position	6.41	6.56	16.54	17.03	18.28	19.49
	Needle beam at the lowest position	6.41	6.57	16.53	17.03	18.27	18.61

It is evident that the height of the position has a great impact on the modal state of the machine, and the lower the height, the lower the first and second order natural frequency. At the same position, the natural frequency of the entire needle punching machine does not change much, i.e., the position of the needle beam does not have much influence on the modal state.

The designed needle punching frequency of this machine reaches 3 Hz. Notably, when the main needle punching module descends to its lowest position during operation, the distance to the crucible preform is the closest, resulting in the maximum elongation of the lead screws. Consequently, the natural frequency at this configuration closely aligns with the needle punching frequency, thereby heightening the risk of resonance within the needle punching apparatus. This specific modal condition is further detailed in the analysis presented in Fig. 3 and Table 3.

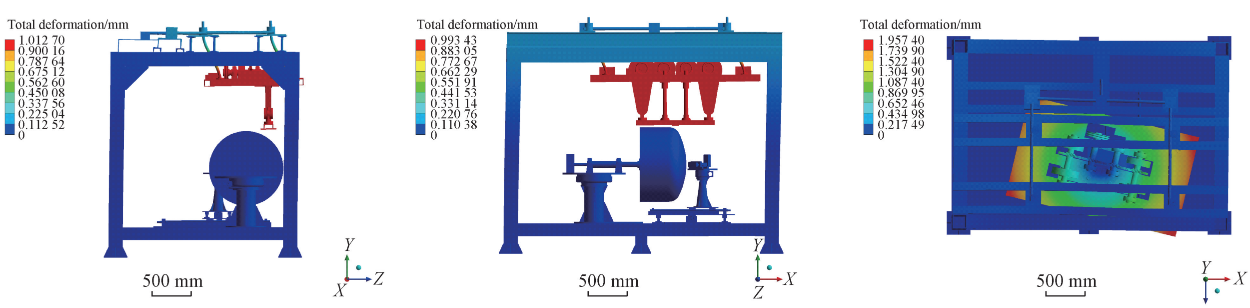

(a) (b) (c)

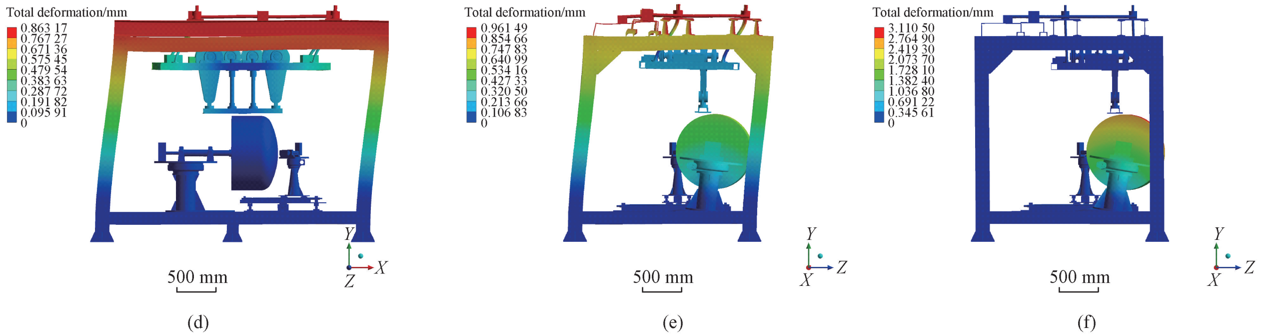

Fig. 3 Vibration mode diagrams for the first six orders before optimization: (a) 1st vibration mode; (b) 2nd vibration mode; (c) 3rd vibration mode; (d) 4th vibration mode; (e) 5th vibration mode; (f) 6th vibration mode

Table 3 The first six natural frequencies and vibration modes of entire needle punching machine

Order	Natural frequency/Hz	Maximum deformation/mm	Vibration mode
1st	6.41	1.01	Main needle punching module swings along the *Z*-axis
2nd	6.57	0.99	Main needle punching module swings along the *X*-axis
3rd	16.53	1.96	Main needle punching module twists around the *Y*-axis
4th	17.03	0.86	Frame swings along the *X*-axis, and main needle punching module twists around the *Y*-axis
5th	18.27	0.96	Frame swings along the *Z*-axis, and the base of the core mold rotational support module swings along the *Z*-axis
6th	18.61	3.11	The base of the core mold rotational support module swings along the *Z*-axis

From the first to third order modal shapes, it can be seen that there is a significant deformation in the connecting lead screw between the main needle punching module and the frame. This is mainly due to the deformation of the lead screw used for lifting the main needle bed. The vibration of the screw here would drive the vibration of the entire main needle punching module. The characteristics of the fourth and fifth order deformation are all manifested as the swing of the frame. The sixth order deformation mainly occurs at the base of the core mold rotational support module. Since the operating frequency of the needle punching machine can be up to 3 Hz, it is close to the first two orders of the natural frequency. Therefore, it is necessary to optimize the structure of the connection between the main needle punching module and the rack.

2.2 Harmonic response analysis of entire needle punching machine

2.2.1 Principles of harmonic response analysis

The displacement from the modal analysis is a relative value, not the actual vibration displacement. It characterizes the relative ratio of the vibration amount of each node at a certain order of the natural frequency, reflecting the transmission of vibration at the natural frequency[15-16]. Because the needle punching machine is subjected to long-term cyclic load, the modal analysis of the needle punching machine is not enough. The harmonic response analysis is also carried out on the basis of modal analysis of the entire needle punching machine. Through the harmonic response analysis, the specific vibration situation of the needle punching machine within a frequency range and the displacement frequency relationship of key nodes in various directions can be obtained. Thus, it can better predict the sustained dynamic characteristics of the needle punching machine and verify whether the design can overcome the harmful effects caused by resonance, fatigue and other forced vibration[17].

The harmonic response analysis focuses on the response of linear structures under periodic excitation. It can solve the steady-state response of the structure under sinusoidal loading and obtain the response and frequency change curves of the structure. Thus it can analyze the stresses and deformations of the structure at the peak frequency. The harmonic response analysis is a linear analysis that ignores nonlinear properties such as plasticity and contact[18]. For the second order system under simple harmonic loading, the differential equation of motion is[19]

$$\boldsymbol{M}\ddot{\boldsymbol{x}} + \boldsymbol{C}\dot{\boldsymbol{x}} + \boldsymbol{K}\boldsymbol{x} = \boldsymbol{F}_1(t)\sin(\theta t), \tag{6}$$

where $\boldsymbol{F}_1(t)$ represents the sinusoidal load; θ represents the excitation frequency.

The displacement response of the node is

$$\boldsymbol{x} = \boldsymbol{A}\sin(\theta t + \psi), \tag{7}$$

where $\boldsymbol{A}$ represents the displacement vector amplitude; ψ represents the phase angle of the displacement response lagging the excitation load.

2.2.2 Results of harmonic response analysis for entire needle punching machine

Based on the results of the modal analysis, in the harmonic response analysis module of ANSYS Workbench, the modal superposition method is used to analyze the harmonic response of the needle punching machine. According to the force state of the needle punching machine during operation, a load of 0 N in the X-axis and Z-axis directions and a load of -1 600 N in the Y-axis direction are applied to the mounting plate of the main needle punching module. This harmonic force is the combined force of an inertia force and a needle piercing force exerted on the main needle bed at the maximum rotational speed.

The modal analysis reveals that the first six low-order natural frequencies range from 6 to 19 Hz. Consequently, the frequency sweep for the harmonic response analysis is set from 0 to 20 Hz. Within this frequency band, 40 solution intervals are defined, with a damping ratio of 0.02. To precisely determine the position of the maximum amplitude, the cluster number is set to be 5. The lower surface of the needle plate of the main needle punching module serves as the designated output position for the response analysis. Figure 4 illustrates the relationship between the vibration amplitude and the excitation frequency at the needle of the main needle plate.

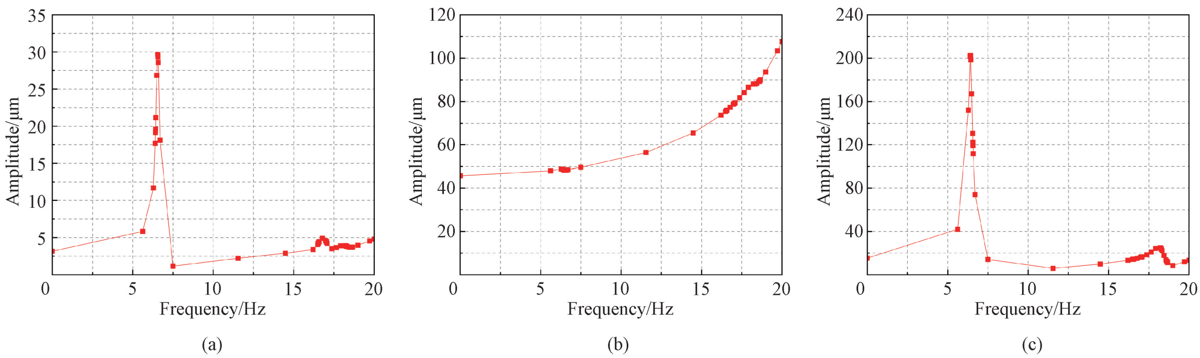

Fig. 4 Harmonic response curve of main needle plate: (a) in X-axis direction; (b) in Y-axis direction; (c) in Z-axis direction

From Fig. 4, it is evident that within a frequency range of 0 to 20 Hz, the amplitude response at the target node exhibits distinct patterns in three directions. Notably, the amplitude gradually increases in the Y-axis direction within this frequency range. The amplitude in the X-axis direction displays peaks at approximately 6.55 and 16.78 Hz, and that in the Z-axis direction displays peaks at approximately 6.55 and 18.22 Hz. The maximum amplitude occurs at around 6.55 Hz. Specifically, the amplitude in the Z-axis direction is the highest, about 202 μm.

The detailed modal analysis indicates that the first peak amplitude corresponds to the first two natural frequencies of the needle punching machine, wherein the needle beam swings along the Z-axis, inducing significant displacements in the Z-axis direction. The second peak amplitude position in the X-axis direction corresponds to the fourth natural frequency of the needle punching machine. The frame swings along the X-axis, and the main needle punching module twists along the Y-axis, causing significant displacement in the X-axis and Z-axis directions. The second peak amplitude position in the Z-axis direction corresponds to the fifth natural frequency of the needle punching machine, and the frame swings along the Z-axis, causing significant displacement in the Z-axis direction. Given that the highest peak in the machine's amplitude spectrum appears at the first two natural frequencies, the machine's dynamic behavior is predominantly influenced by these frequencies. Therefore, it is crucial to circumvent operating at these frequencies during practical applications.

3 Structural Optimization Analysis of Entire Needle Punching Machine

3.1 Structural improvements of key parts

According to Eq. (5), it can be seen that the natural frequency depends only on the material parameters and shape and size of the parts, and is independent of the external load[20]. The natural frequency can be changed by changing only the stiffness and mass conditions. Based on the mechanical system dynamics, increasing the natural frequency of each order of the system can improve the dynamic performance of the structure and optimize the distribution of the inertial energy[21].

According to the previous analyses, the structural integrity and dynamic performance of the entire needle punching machine should be enhanced, particularly at the junction between the main needle punching module and the frame. To address this, a guiding mechanism has been implemented at this junction to increase its stiffness while ensuring practical installation feasibility. This enhancement involves incorporating three guide posts aligned with the lead screw's movement direction, complemented by linear bearings. The refined configuration is illustrated in Fig. 5.

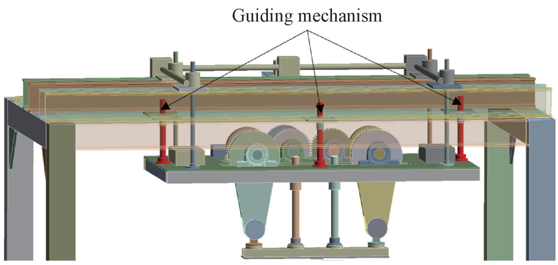

Fig. 5 Improved local 3D model of needle punching machine

3.2 Validation of improved model

Finite element modeling of the optimized needle punching machine is established and the dynamic characteristic analysis is conducted under the same conditions as the original model. The results are shown in Fig. 6. The comparison of the natural frequency, deformation and vibration mode of the entire needle punching machine before and after optimization is shown in Tables 4 and 5. Additionally, the results of the harmonic response analysis after optimization are visually represented in Fig. 7.

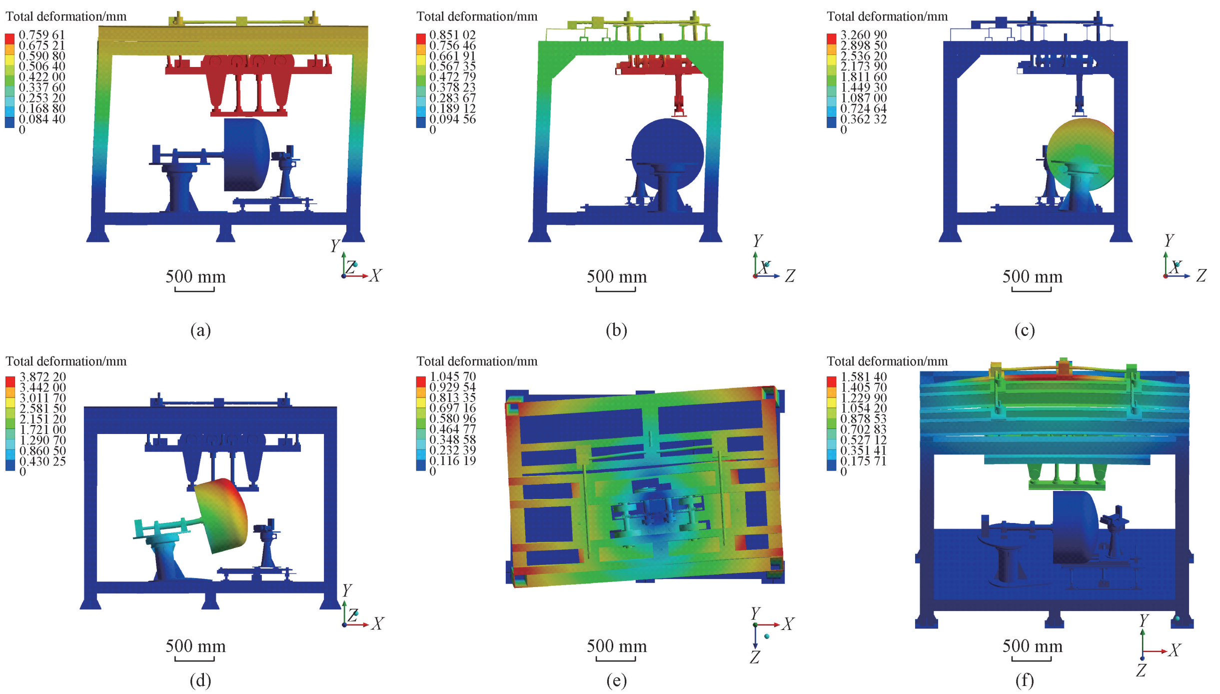

Fig. 6 Vibration mode diagrams for the first six orders after optimization: (a) 1st vibration mode; (b) 2nd vibration mode; (c) 3rd vibration mode; (d) 4th vibration mode; (e) 5th vibration mode; (f) 6th vibration mode

Table 4 Comparison of the first six natural frequencies and maximum deformations of entire needle punching machine before and after optimization

Order	Before optimization		After optimization		Rate of change/%	
	Natural frequency/Hz	Maximum deformation/mm	Natural frequency/Hz	Maximum deformation/mm	Natural frequency	Maximum deformation
1st	6.41	1.01	10.92	0.76	70.4	−24.8
2nd	6.57	0.99	11.85	0.85	80.4	−14.1
3rd	16.53	1.96	19.49	3.26	17.9	66.3
4th	17.03	0.86	21.51	3.87	26.3	350.0
5th	18.27	0.96	23.05	1.05	26.2	8.6
6th	18.61	3.11	25.72	1.58	38.2	−49.2

Table 5 Comparison of the first six vibration modes of entire needle punching machine before and after optimization

Order	Before optimization	After optimization
1st	Main needle punching module swings along the *Z*-axis	Frame swings along the *X*-axis
2nd	Main needle punching module swings along the *X*-axis	Frame swings along the *Z*-axis
3rd	Main needle punching module twists around the *Y*-axis	The base of the core mold rotational support module twists around the *X*-axis
4th	Frame swings along the *X*-axis, and main needle punching module twists around the *Y*-axis	The base of the core mold rotational support module twists around the *Z*-axis
5th	Frame swings along the *Z*-axis, and the base of the core mold rotational support module swings along the *Z*-axis	Frame twists around the *Y*-axis
6th	The base of the core mold rotational support module swings along the *Z*-axis	The top of the frame with the main needle punching module swings up and down along the *Y*-axis

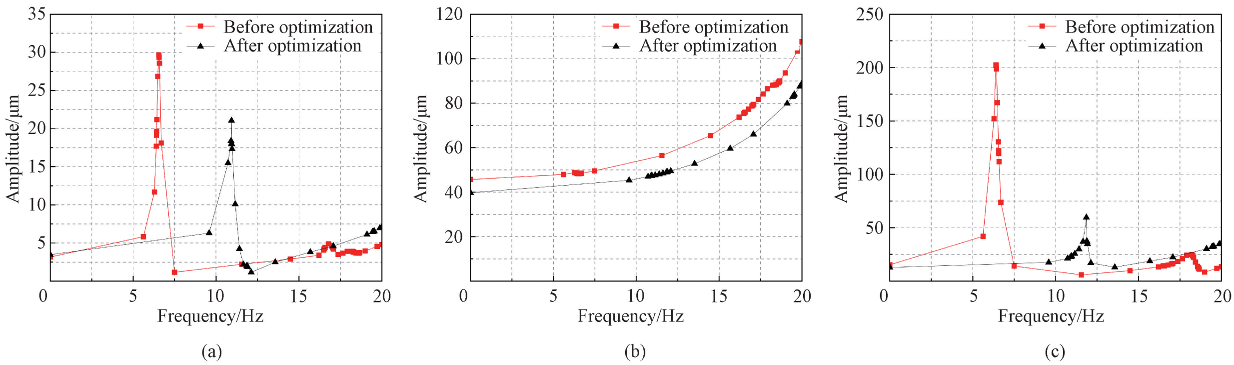

Fig. 7 Harmonic response curves of main needle plate after optimization: (a) in *X*-axis direction; (b) in *Y*-axis direction; (c) in *Z*-axis direction

The first two natural frequencies of the entire needle punching machine increase from 6 Hz to around 11 Hz. The first order natural frequency of the optimized machine increases by 70.4%, and the second order natural frequency increases by 80.4%, effectively circumventing the needle punching machine's operating frequency of 3 Hz and reducing resonance risks. The reduction in the maximum deformation in Figs. 6 (a) and 6 (b) suggests enhanced stability of the main needle punching structure. The harmonic response curve of the optimized machine reveals that the highest amplitudes in the *X*-axis and *Z*-axis directions occur at 10.89 and 11.81 Hz, respectively. The maximum amplitude in the *X*-axis direction decreases from 30 to 21 μm, a reduction of 30%. The maximum amplitude in the *Z*-axis direction decreases from 202 to 60 μm, a reduction of 70.3%. The amplitude in the *Y*-axis direction also decreases within this frequency range. These improvements demonstrate a significant enhancement in the vibration-resistant performance of the needle punching machine under dynamic interference excitation. The comprehensive improvement in the dynamic characteristics of the entire needle punching machine achieves the intended optimization goals.

4 Conclusions

To address the issue of severe vibration in the needle punching process of the entire double-shaft-driven needle punching machine for C/C crucible preforms, the dynamic characteristic analysis and optimization have been conducted. The modal analysis of the entire needle punching machine has identified the connection between the main needle punching module and the frame as a structural weak point. Upon the harmonic response analysis, the harmonic response curve of the machine under a simple harmonic load reveals that the machine's amplitude is relatively high when the excitation load frequency is close to the first-order natural frequency. Consequently, structural optimization of these weak parts has been implemented, resulting in a significant increase in the first six orders of natural frequencies and effectively circumventing the operating frequency. This optimization strategy not only meets design and manufacturing requirements but also is straightforward to implement, showcasing a high degree of feasibility. The enhanced stiffness and overall performance of the optimized needle punching machine offer a robust theoretical foundation for the future design and production of entire double-shaft-driven needle punching machines for C/C crucible preforms.

References

[1] LI C S, LIU Q L. Analysis of the patent status of China's monocrystalline silicon production process[J]. *Advanced Materials Industry*, 2019(9): 61-64. (in Chinese)

[2] WANG Z X, REN Y S, MA W H, et al. Principle, process and prospect of monocrystalline silicon growth with Czochralski method[J]. *Material Reports*, 2024, 38(9): 5-17. (in Chinese)

[3] WANG J J, WU F Z, WU J X, et al. Research on the mechanism model of carbon composite material damaged by erosion in the thermal field of single crystal silicon furnace[J]. *Earth and Environmental Science*, 2021, 632(5): 52089.

[4] TONG H T. Improvement of the design of the needle punching mechanism of the pre-burring machine[J]. *Machinery Design & Manufacture*, 2002(2): 72-73. (in Chinese)

[5] XU T. Analysis and discussion on vibration and noise of needle punching machine[J]. *Progress in Textile Science & Technology*, 2019(10): 12-17. (in Chinese)

[6] ZHONG X Q, JI Q Q, JI L Z, et al. Simulation analysis of the bed of needling machine producing high gram weight nonwovens [J]. *IOP Conference Series: Materials Science and Engineering*, 2019, 585(1): 012113.

[7] YUN Y P. Application of computer simulation technology in modal analysis of engine mount [J]. *Vibroengineering Procedia*, 2023, 52: 74-80.

[8] ZHANG J D. Electromechanical coupling modeling and dynamic characteristics analysis of machinetool dual-drive feed system [D]. Hangzhou: Hangzhou Dianzi University, 2024. (in Chinese)

[9] XIE J H. Research on slider-crank mechanism dynamic characteristics of needling machine[D]. Xi'an: Xi'an Polytechnic University, 2012. (in Chinese)

[10] WANG X W. Modal analysis and structural optimization of water valve bracket based on ANSYS Workbench[J]. *Agricultural Equipment & Vehicle Engineering*, 2024, 62(5): 66-69. (in Chinese)

[11] MA Y L. The research of structure modal analysis realization [D]. Hangzhou: Zhejiang University, 2008. (in Chinese)

[12] LIU W Z, HUANG M J, LI W G, et al. Dynamic analysis on the main transmission device of wooden ice cream sticks branding machine [J]. *Journal of Donghua University (English Edition)*, 2019, 36(3): 234-238.

[13] LIU B, ZHAO Y G. Overall structure design and modal analysis of turnover machine in tile packaging production line[J]. *Modular Machine Tool & Automatic Manufacturing Technique*, 2017(9): 136-138. (in Chinese)

[14] DONG X, GAO T H. The research on dynamic response of three DOF parallel machine tool[J]. *Modular Machine Tool & Automatic Manufacturing Technique*, 2018(11): 30-33, 42. (in Chinese)

[15] LIU J J, YIN M D, ZHANG Z L. Modal and harmonic analysis based on ANSYS for light helicopter tail beam tube [J]. *Mechanical Engineering & Automation*, 2013(1): 64-66. (in Chinese)

[16] LI C Q, YANG W C, YANG H, et al. Modal and harmonic response analysis for the rack of *notoginseng* sowing machine base on ANSYS [J]. *Manufacturing Automation*, 2015(7): 77-79. (in Chinese)

[17] LIU T, YANG F P. Proficient in ANSYS[M]. Beijing: Tsinghua University Press, 2002: 323-344. (in Chinese)

[18] SAMANTA K, MAHESHWARI P. Effect of negative phase of pulse loading on response of machine foundations vibrating under harmonic loads[J]. *Mechanics Based Design of Structures and Machines*, 2023, 51(11): 6008-6022.

[19] ZHENG B, E J Y. Finite element modal analysis and harmonic response analysis of engine connecting rod[J]. *Journal of Machine Design*, 2020, 37(Sup. 1): 98-101. (in Chinese)

[20] MA X S, LUO F F. The static & dynamic characteristic analysis and topology optimization of the column in gantry vertical machining center [J]. *Gansu Science and Technology*, 2021, 37(2): 45-49. (in Chinese)

[21] HU S J, LI Z X. Dynamic characteristic analysis and optimization of machine tool based on inertial energy distribution [J]. *Machine Design and Manufacturing Engineering*, 2021, 50(2): 65-69. (in Chinese)

双轴驱动 C/C 坩埚预制体针刺机整机动态特性分析及结构优化

孙志宏[1*]，邓奇才[1]，曲志洋[1]，王振喜[2]，王　兵[2]，张　喜[1]，张竞章[2]

1. 东华大学 机械工程学院，上海 201620

2. 航宸石家庄新材料科技有限公司，河北 石家庄 051432

摘　要：双轴驱动 C/C 坩埚预制体针刺机是加工 C/C 坩埚预制体的专用设备，其主针刺模块由两套作往复运动的曲柄滑块机构驱动，在针刺过程中产生剧烈振动。振动不仅会产生较大的噪声，而且会严重降低预制体针刺质量，因此需对针刺机进行整机动态特性分析和优化以减少振动。该文建立双轴驱动 C/C 坩埚预制体针刺机三维模型。基于模态分析理论，对多个工况下针刺机的模态进行分析，确定其固有频率及振型。通过谐响应分析得到针板在不同频率下的振幅，确认针刺机结构的薄弱环节并进行优化，分析和验证优化后方案的可行性。结果表明：结构优化后针刺机的前六阶固有频率均有提升，针板最大振幅降低 70.3%，整机动态特性良好，能更好地实现对 C/C 坩埚预制体的针刺。

关键词：针刺机；动态特性；模态分析；谐响应分析；结构优化